

# Electro-Responsively Reversible Transition of Polythiophene Films from Superhydrophobicity to Superhydrophilicity

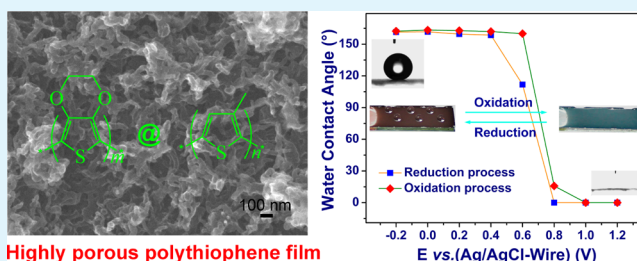
Lianyi Xu, Qiang Ye, Xuemin Lu, and Qinghua Lu\*

School of Chemistry and Chemical Engineering, Shanghai Jiao Tong University, Shanghai 200240, People's Republic of China

## Supporting Information

**ABSTRACT:** An electro-responsively reversible switching of wettability between superhydrophobicity and superhydrophilicity has been obtained from a highly porous structured polythiophene film. The polythiophene film was prepared by two-step electrochemical deposition on an indium tin oxide (ITO) substrate. The underlying poly(3,4-ethylenedioxythiophene) (PEDOT) provides a highly porous structured conductive support, and poly(3-methylthiophene) (P(3-MTH)) deposited thereon plays the role of a low-surface-energy conductive coating. The wettability switching of this double-layer film between superhydrophobicity and superhydrophilicity has been investigated by doping and dedoping in an electrolyte solution containing  $\text{ClO}_4^-$ . Electrochromism of the film was also seen to accompany the electrochemical process of conversion between the two superwetting states. On the basis of this porous electro-active film, an in situ electro-wetting device was also demonstrated.

**KEYWORDS:** polythiophene film, wettability transition, superhydrophobicity, superhydrophilicity, surface chemistry



## 1. INTRODUCTION

Control of surface wettability is of considerable technological and scientific importance, with applications in self-cleaning surfaces,<sup>1–7</sup> antifogging surfaces,<sup>8,9</sup> microfluid systems,<sup>10,11</sup> and biotechnology.<sup>12</sup> Surface wettability is usually governed by the surface geometry and chemical composition.<sup>1,5,13</sup> Smart surfaces with reversibly switchable wettability have received special attention due to their vital importance in many fields. Such surfaces may be constructed by introducing a stimuli-responsive material into an appropriately rough structure,<sup>14–19</sup> and the reversible switching feature can be realized with the help of an external stimulus such as light irradiation,<sup>20–22</sup> temperature,<sup>18</sup> pH,<sup>23</sup> solvent,<sup>19,24</sup> or electrical potential.<sup>25–28</sup> Among stimuli-responsive materials,  $\pi$ -conjugated polymers are typical electrochemical-responsive materials and can be easily prepared.<sup>17,27,29,30</sup> In particular, for  $\pi$ -conjugated polymers that can be doped (oxidized) and dedoped (reduced) by applying a voltage in an electrolyte solution, these processes are accompanied by counterions (dopants) moving into and out of the film. This may result in a conversion of the wetting properties of the  $\pi$ -conjugated polymer. Yan et al. employed perfluorooctanesulfonate to dope polypyrrole (PPy) film, which resulted in a change in surface wetting from superhydrophilicity to superhydrophobicity.<sup>17</sup> Advincula et al. electrochemically polymerized a polythiophene derivative, poly(GO–3T COOR), as a surface layer on polystyrene (PS) nanoparticles, and found that the wetting could be switched by doping and dedoping of tetrabutylammonium hexafluorophosphate.<sup>27</sup> Although highly porous structures of  $\pi$ -conjugated polymer films were successfully achieved in these two studies, which is necessary

not only for the passage of counterions but also for the amplification of surface wettability properties,<sup>17,31–36</sup> the processes are complicated and additional substances need to be added. This may cause a reduction in the transparency of the film or a weakening of the adhesion between the polymer layer and conductive substrate. For example, in previous work,<sup>17</sup>  $\text{Fe}^{3+}$  was included as catalyst in the plating solution, and coupling of electropolymerization and  $\text{Fe}^{3+}$ -catalyzed chemical polymerization promoted the growth of a porous, rough PPy film. In the second study,<sup>27</sup> the latex assembly of PS nanoparticles on a flat conducting substrate was first carried out by an LB-like technique, and then the polythiophene derivative was electro-deposited to form a rough polymer surface. The required roughness of the PS nanoparticles may have reduced the conductivity of the electrochemically deposited film. Therefore, such electro-active  $\pi$ -conjugated polythiophene films, which are easy to prepare on a large scale, have remained unexplored for wetting switching application.

In our earlier study, an electro-responsive double-layer polythiophene film was prepared for water-droplet adhesion switching reversibility between sliding and pinned superhydrophobic states.<sup>37</sup> This preparation process did not need any additive for the creation of a rough surface and low surface energy. Poly(3,4-ethylenedioxythiophene) (PEDOT) was directly electrodeposited on an indium tin oxide (ITO)-coated glass electrode to provide a porous conducting substrate. On

Received: July 4, 2014

Accepted: August 12, 2014

Published: August 12, 2014

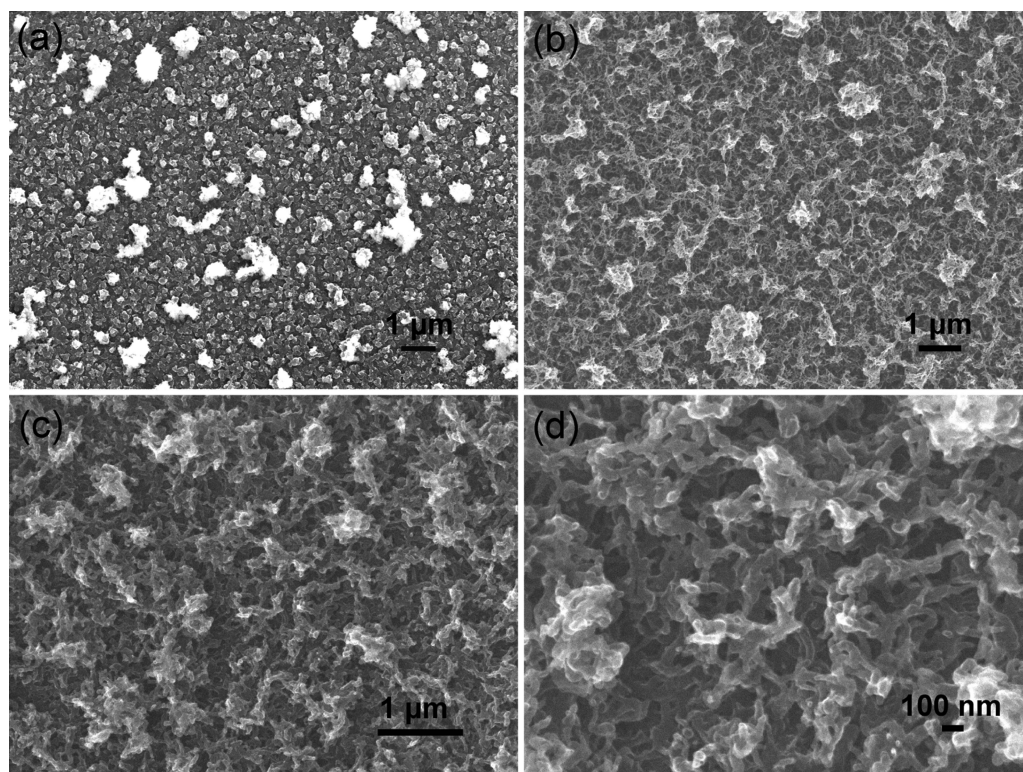


**Figure 1.** Scanning electron microscopy (SEM) image of the electrodeposited films: (a) P(3-MTH) film, (b) highly porous network-like PEDOT film, and (c) highly porous PEDOT-P(3-MTH) film. (d) Magnified image of PEDOT-P(3-MTH) showing the network-like nanostructure.

the surface of the porous PEDOT, hydrophobic poly(3-hexylthiophene) (P(3-HTH)) was further electrodeposited. Such double-layer polythiophene possesses a strongly superhydrophobic surface both at doping and dedoping, that is, their static water contact angle (WCA) is always greater than  $150^\circ$ , which provides a good platform for the preparation of adhesion switching (sliding angle (SA) changes between  $0^\circ$  and  $>90^\circ$ ). Different to the above-mentioned work, in this work, we focused on an electro-responsive wetting switching reversible between superhydrophobicity and superhydrophilicity (WCA changes between  $>150^\circ$  and  $\sim 0^\circ$ ). Thereby, the overlying polythiophene P(3-HTH) was replaced by another polythiophene with a shorter alkyl group, poly(3-methylthiophene) (P(3-MTH)), to moderately tune the hydrophobicity of double-layer film. The obtained double-layer polythiophene film (PEDOT-P(3-MTH)) exhibited superhydrophobicity with a WCA  $> 150^\circ$ . Through continuously doping and dedoping at redox potentials, the as-prepared PEDOT-P(3-MTH) film displayed a reversible conversion between superhydrophilicity at the doped state and superhydrophobicity at the dedoped state. This wettability switching has been investigated by precisely adjusting the doping and dedoping potentials.

## 2. EXPERIMENTAL SECTION

**2.1. Materials.** Commercial high-performance liquid chromatography grade acetonitrile (ACN) was provided by Shanghai Lingfeng Chemical Reagent Company and was used without further purification. 3,4-Ethylenedioxythiophene (EDOT), 3-methylthiophene (3-MTH), anhydrous lithium perchlorate ( $\text{LiClO}_4$ ), and tetrabutylammonium hexafluorophosphate ( $(\text{CH}_3\text{CH}_2)_4\text{N}^+\text{PF}_6^-$ , TBAHF) were purchased from Aladdin.

**2.2. Characterization.** Field-emission scanning electron microscopy (FE-SEM) was performed with a Nova NanoSEM instrument

(FEI, Hillsboro, OR). Static water contact angle measurements were performed by the sessile drop method on a Contact Angle System OCA 20 (DataPhysics Instruments GmbH, Germany) in air. The contact angles reported herein are mean values measured for  $4 \mu\text{L}$  water droplets at five different positions on each sample. Water SAs were determined by slowly tilting the sample stage until a  $4 \mu\text{L}$  water drop started moving. The chemical compositions of the surfaces were determined by X-ray photoelectron spectroscopy (XPS) on a Kratos Axis Ultra DLD spectrometer (Kratos Analytical, Ltd., Manchester, U.K.) with a monochromated Al K $\alpha$  radiation source (1486.6 eV) and a takeoff angle of  $90^\circ$ . UV/vis spectra of the films on the ITO substrate were measured on a PerkinElmer Lambda 20 UV/vis spectrometer. Photographs and movies were taken with a camera.

**2.3. Electrochemical Synthesis and Experiments.** All electrochemical experiments were performed in an electrochemical cell ( $1 \times 1 \times 4.5 \text{ cm}$ ) with a three-electrode system by using a computer-controlled CHI 630E Electrochemical Analyzer. The working electrode was ITO glass ( $<10 \Omega \text{ sq}^{-1}$ ,  $0.9 \times 5 \text{ cm}$ ), which was washed successively under ultrasonication with deionized water and absolute ethanol and then dried with a stream of  $\text{N}_2$  before use. The counter electrode was a platinum wire (1 mm diameter), which was cleaned before each examination. An Ag/AgCl wire was used as a quasi-reference electrode. All electrochemical experiments were performed at room temperature and  $<40\%$  relative humidity. Polythiophene films were electrodeposited on ITO electrodes by cyclic voltammetry (CV) in ACN solution containing 0.2 M  $\text{LiClO}_4$  as the supporting electrolyte. All films were rinsed twice with ACN ( $2 \times \text{ca. } 1 \text{ mL}$ ) and then dried at room temperature for several minutes under flowing  $\text{N}_2$  before characterization.

**2.4. Electrochemical Preparation of P(3-MTH).** A P(3-MTH) film was directly electrodeposited by CV onto a smooth ITO glass substrate of 0.05 M 3-MTH electrolyte solution between 0 and +1.9 V or at constant potential (+1.9 V;  $Q \approx 330.9 \pm 20 \text{ mC cm}^{-2}$ ) (Figure S1, Supporting Information). The P(3-MTH) could be doped at +1.2 V (oxidation) and dedoped at 0 V (reduction) in ACN solution containing  $\text{LiClO}_4$  as the supporting electrolyte.

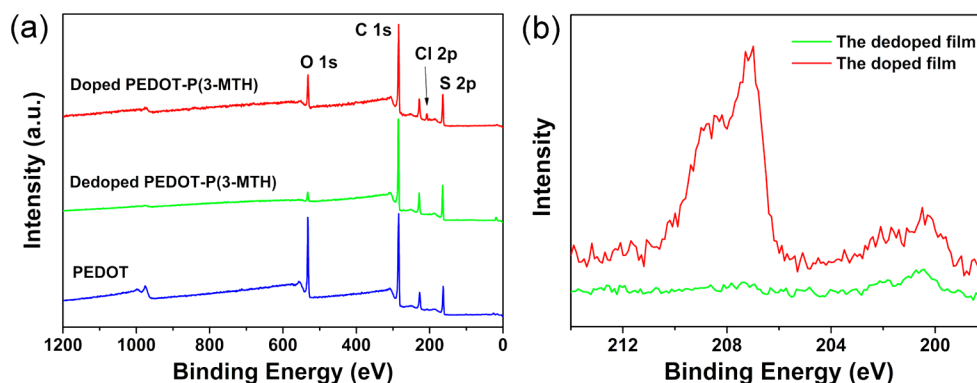


**Figure 2.** (a) XPS spectra of the (blue) dedoped PEDOT, and PEDOT-P(3-MTH) in the (green) dedoped and (red) doped states. (b) High-resolution XPS spectra of Cl (2p, 207.0 eV) in the (green) dedoped and (red) doped PEDOT-P(3-MTH).

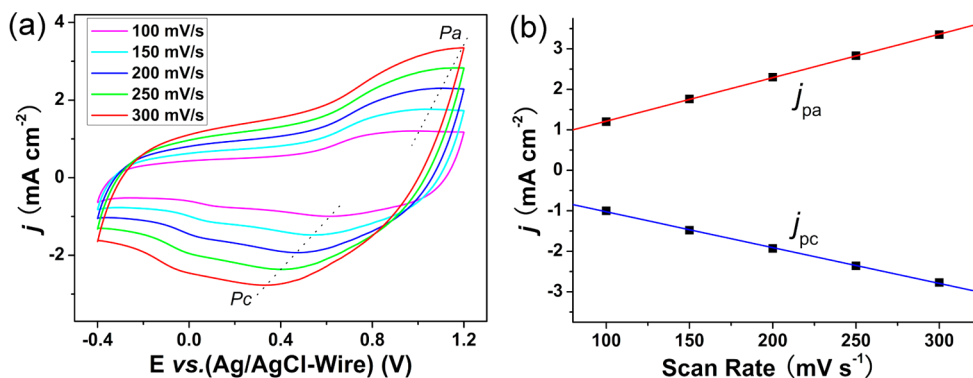


**Figure 3.** (a) Cyclic voltammograms of PEDOT-P(3-MTH) in monomer-free 0.2 M LiClO<sub>4</sub>/ACN solution at scan rates between 100 and 300 mV s<sup>-1</sup>. (b) Peak current density ( $j_{pa}$  and  $j_{pc}$ ) vs scanning rate;  $j$  denotes the current density; pa and pc denote the oxidation peak and the reduction peak, respectively.

**2.5. Electrochemical Preparation of PEDOT-P(3-MTH).** An underlying film of PEDOT was first electrodeposited by CV of a 0.01 M EDOT electrolyte solution between  $-0.7$  and  $+1.6$  V, applying an electrodeposition charge ( $Q$ ) of about  $32.5 \pm 2$  mC cm<sup>-2</sup> (Figure S2a, Supporting Information). Thereafter, a poly(3-methylthiophene) P(3-MTH) film was electrodeposited on the as-prepared PEDOT film by CV of a 0.05 M 3-MTH solution between  $-0.4$  and  $+1.9$  V, with  $Q \approx 64.2 \pm 5$  mC cm<sup>-2</sup> (Figure S2b, Supporting Information). Notably, a low-adhesion superhydrophobic film could only be obtained when the electrodeposition charge used to apply the surface P(3-MTH) moieties was nearly twice that used for the underlying PEDOT moieties. The constant-potential method was applied for doping (at  $+1.2$  V for 5 s) and dedoping (at  $-0.2$  V for 10 s) of PEDOT-P(3-MTH) in monomer-free electrolyte solutions.

**2.6. Electrochemical Characterization of the Films.** The electrochemical properties of the as-prepared PEDOT-P(3-MTH) in electrolyte solution were characterized by sweeping potentials of  $-0.4$  to  $+1.2$  V at scan rates between 100 and 300 mV s<sup>-1</sup>. Cyclic voltammograms of the as-prepared PEDOT-P(3-MTH), PEDOT, and P(3-MTH) films in electrolyte solution were obtained at a scan rate of 200 mV s<sup>-1</sup>.

**2.7. Electrochemical Properties of PEDOT-P(3-MTH) Film in TAHFP/ACN Solution.** The CV curve of PEDOT-P(3-MTH) film in a 0.2 M TAHFP/ACN solution was created by scanning the potential from  $-0.4$  to  $+1.6$  to  $-0.4$  V with a scan rate of 200 mV s<sup>-1</sup>. In this electrolyte system, PEDOT-P(3-MTH) film was doped with TAHFP (the counterion is PF<sub>6</sub><sup>-</sup>) at an oxidation potential of  $+1.6$  V for 5 s and dedoped at a reduction potential of  $-0.2$  V for 10 s. The WCAs of the doped and dedoped film were measured after rinsing the film with ACN ( $2 \times$  ca. 1 mL) and then drying it at room temperature for several minutes under flowing N<sub>2</sub>.

**2.8. Electro-Wetting Properties of PEDOT-P(3-MTH) Device under the Transition Potential.** A simple electro-wetting device

comprised a porous PEDOT-P(3-MTH) film and a water droplet containing 0.2 M LiClO<sub>4</sub> sitting on the film. The water droplet was linked to the counter (negative) electrode by a 1 mm diameter platinum wire, and the film was linked to the work (positive) electrode. The electro-wetting test was done using a transition potential of  $+1.5$  V between the water droplet and the PEDOT-P(3-MTH) film. The water droplet change in WCA with time prolonging was recorded using a Contact Angle System OCA 20.

### 3. RESULTS AND DISCUSSION

**3.1. Morphology and Chemical Composition of PEDOT-P(3-MTH).** In general, electrodeposited polythiophenes with short alkyl side chains (typically  $n \leq 6$  in C<sub>n</sub>H<sub>2n+1</sub> groups) do not provide sufficient roughness to support a superhydrophobic/superhydrophilic conducting surface.<sup>37–39</sup> For example, the surface topography of electrodeposited P(3-MTH) is shown in Figure 1a. This P(3-MTH) film displayed only a wettability change from hydrophobicity (WCA of  $115.2^\circ \pm 5^\circ$ ) to hydrophilicity ( $35.5^\circ \pm 5^\circ$ ) after doping it with LiClO<sub>4</sub> at an appropriate oxidation potential (Figure S3, Supporting Information). However, an electrodeposited PEDOT film has a highly porous network-like structure (electrodeposition charge ( $Q$ ) = 32.5 mC cm<sup>-2</sup>), as shown in Figure 1b, which is highly advantageous for the preparation of a conductive super wetting coating. To this end, a double-layer PEDOT-P(3-MTH) film was prepared by sequentially electrodepositing PEDOT and P(3-MTH) on the same ITO electrode from respective monomer-containing LiClO<sub>4</sub>/ACN solutions (see curves obtained by CV in Figure S2 Supporting Information). The highly porous and nanoscale rough structure

of PEDOT was successfully retained after the electrodeposition of P(3-MTH) ( $Q = 64.2 \text{ mC cm}^{-2}$ ; Figure 1c). This result can be attributed to the growth-orienting effect of the network structure of the PEDOT film.<sup>37</sup> A magnified image shows that the porous structure is composed of conductive polymer fibers of about 100 nm (Figure 1d). This method for the preparation of highly porous nanostructured  $\pi$ -conjugated polymer films may also be used in other photoelectrical fields.<sup>40</sup> The surface chemical composition of PEDOT–P(3-MTH) was determined by XPS (Figure 2a). The relative intensity of the photoelectron peak of O (1s, 532.8 eV) in the spectrum of PEDOT–P(3-MTH) is significantly lower than that in the spectrum of the PEDOT film, confirming that the outermost layer of the PEDOT–P(3-MTH) structure is mainly composed of hydrophobic P(3-MTH) moieties.

### 3.2. Electrochemical Properties of PEDOT–P(3-MTH).

The electrochemical properties of PEDOT–P(3-MTH) were examined. PEDOT–P(3-MTH) showed a strong electrochemical response (Figure 3a), and the peak current densities [ $j$ , redox peak pairs at the oxidation peak (pa) and the reduction peak (pc)] were proportional to the potential scan rates (Figure 3b), indicating the reversible redox process in this film.<sup>41</sup> This result indicates that the as-prepared PEDOT–P(3-MTH) retained the high redox activity of polythiophenes.

### 3.3. Reversible Wettability Switching under the Application of a Potential.

The as-prepared PEDOT–P(3-MTH) could be reversibly doped and dedoped under oxidation and reduction potentials, respectively, in an electrolyte solution containing  $\text{ClO}_4^-$  (Figure 4a). The WCAs in the doped and dedoped states of the PEDOT–P(3-MTH) film were measured (Figure 4b). Upon dedoping at a potential of  $-0.2 \text{ V}$ , this film displayed superhydrophobicity, as evidenced by a high static WCA of  $162.4^\circ \pm 2^\circ$  and a low water sliding angle of  $3.0^\circ \pm 1^\circ$  (Figure 4b, left, and Movie S1, Supporting Information). Compared with the hydrophobic P(3-MTH) film (Figure S3b, left, Supporting Information), the highly porous structure of the PEDOT–P(3-MTH) film significantly enhanced the hydrophobicity of the surface P(3-MTH) moieties due to the proportional increase of air/water contact interfaces (in a Cassie state).<sup>31,32,38</sup> Notably, the hydrophobicity of PEDOT–P(3-MTH) film is also higher than that of our earlier PEDOT–P(3-MTH) film (its WCA is about  $159.0^\circ$ ).<sup>37</sup> This result may be attributed to their morphology differences. Although P(3-MTH) has a shorter alkyl side chain, its double-layer film processes more abundant nanostructures, which can reduce the contact area between the water droplet and the interface.<sup>31,32,38</sup> On the contrary, a superhydrophilic PEDOT–P(3-MTH) film could be obtained simply by doping the double-layer film at  $+1.2 \text{ V}$  for 5 s in an electrolyte solution containing  $\text{ClO}_4^-$ . A water droplet spread rapidly on the doped PEDOT–P(3-MTH) film, resulting in a WCA of essentially  $0^\circ$  (Figure 4b, right). The results indicate that the wettability of the PEDOT–P(3-MTH) film changed from superhydrophobicity to superhydrophilicity upon applying the oxidation potential.

With regard to the mechanism of the wetting switching, we propose that upon doping at  $+1.2 \text{ V}$ , the dopant  $\text{ClO}_4^-$  is introduced into the positively charged polythiophene backbones of PEDOT–P(3-MTH) to counterbalance the charge, leading to the formation of a large number of hydrophilic dipoles (Figure 4a).<sup>17,41</sup> A high-resolution XPS spectrum clearly showed that the unique photoelectron peak of Cl (2p, 207.0 eV) was only observed for the doped PEDOT–P(3-MTH) film and not for the dedoped film (Figure 2b). This

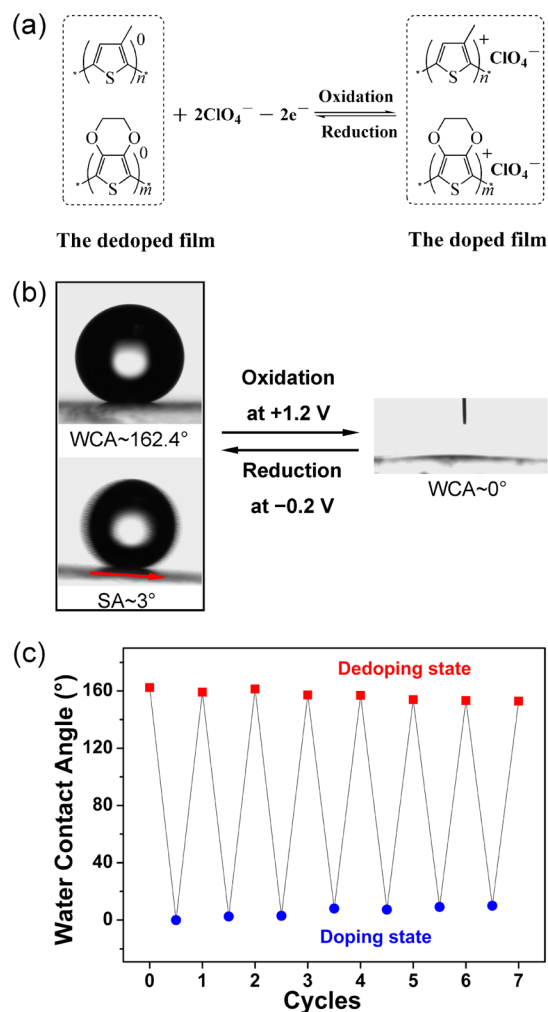


**Figure 4.** (a) Doping (oxidation) and dedoping (reduction) of PEDOT–P(3-MTH) in  $\text{LiClO}_4/\text{acetonitrile}$  solution at potentials between  $+1.2$  and  $-0.2 \text{ V}$ . (b) WCA switching of the PEDOT–P(3-MTH) film between  $162.4^\circ \pm 2^\circ$  (left, top) and ca.  $0^\circ$  upon the alternate application of potentials of  $-0.2$  (reduction) and  $+1.2 \text{ V}$  (oxidation), respectively. In the dedoped state, the film has a low sliding angle of  $3.0^\circ \pm 1^\circ$  (left, bottom). (c) Reversible wettability transition of the PEDOT–P(3-MTH) film between superhydrophobicity (dedoped state) and superhydrophilicity (doped state).

result confirmed that the dopant  $\text{ClO}_4^-$  was only present in the doped PEDOT–P(3-MTH) film. The doping process altered the chemical composition of the film surface, triggering a wettability transition from hydrophobic to hydrophilic.<sup>17,27</sup> When a water droplet was deposited on such a doped and highly porous structured film, it could rapidly fill the inner air pores beneath it due to a two- or three-dimensional capillary effect<sup>14,42,43</sup> and consequently showed an ultralow contact angle. Upon dedoping of the PEDOT–P(3-MTH) film at  $-0.2 \text{ V}$  for 10 s, the polythiophene backbones of the film returned to their neutral state, and the dopant  $\text{ClO}_4^-$  was released back into the electrolyte solution.<sup>17,41</sup> A water droplet deposited on this film exhibited a near-spherical shape with a WCA of more than  $150^\circ$ , indicating that the dedoped film regained its superhydrophobic state. Therefore, reversible switching of the wettability between superhydrophobicity and superhydrophilicity on the PEDOT–P(3-MTH) film was realized by alternately applying potentials of  $-0.2 \text{ V}$  and  $+1.2 \text{ V}$ . As

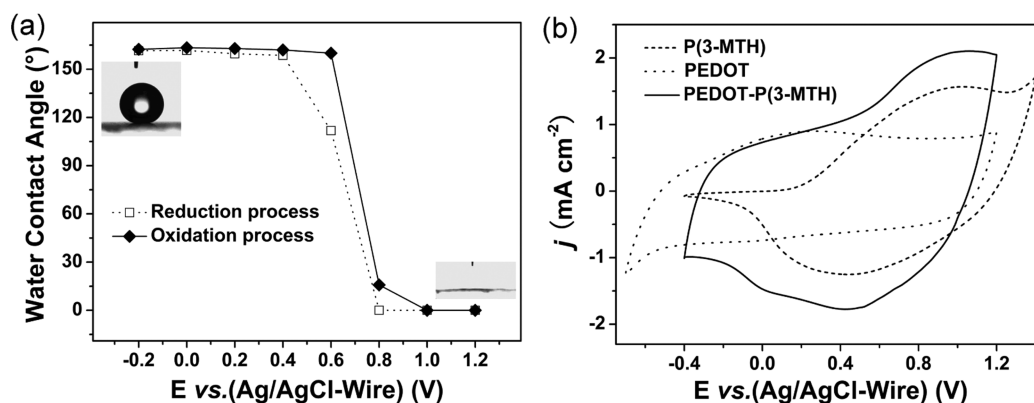


**Figure 5.** (a) WCA measurements on PEDOT-P(3-MTH) under different potentials and the changes in WCA during the increase (◆, oxidation process) and decrease (□, reduction process) in potential between  $-0.2$  and  $+1.2$  V. (b) Cyclic voltammograms of the PEDOT-P(3-MTH), P(3-MTH), and PEDOT films obtained at a scan rate of  $200 \text{ mV s}^{-1}$ ;  $j$  denotes the current density.

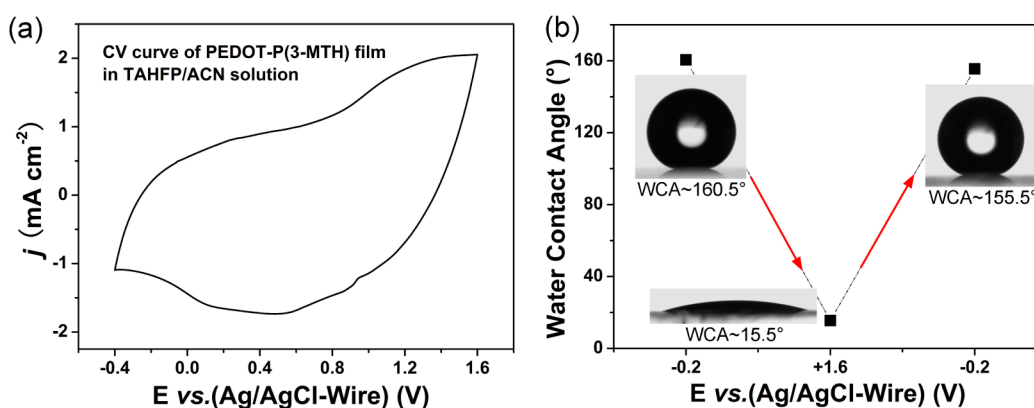


**Figure 6.** (a) Cyclic voltammogram of the PEDOT-P(3-MTH) film obtained at a scan rate of  $200 \text{ mV s}^{-1}$  in a  $0.2 \text{ M TAHPF/ACN}$  solution;  $j$  denotes the current density. (b) The WCAs of the film after doping at  $+1.6$  V and dedoping at  $-0.2$  V in the  $0.2 \text{ M TAHPF/ACN}$  solution.

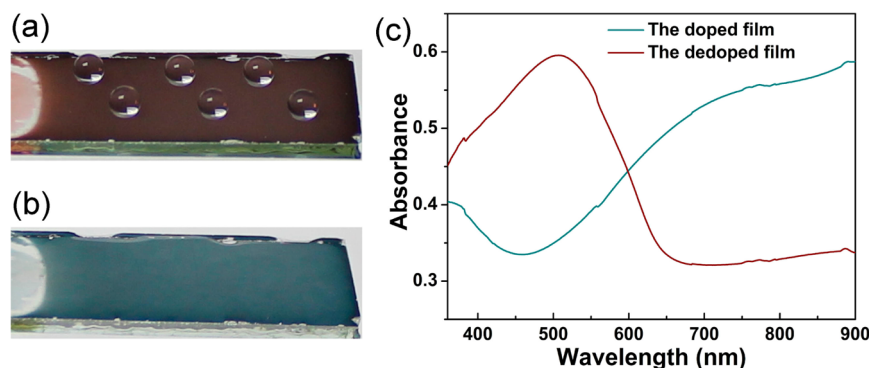


**Figure 7.** (a) Randomly distributed water droplets ( $4 \mu\text{L}$ ) on the reddish brown PEDOT-P(3-MTH) film. These water droplets show almost spherical shape. (b) Doped PEDOT-P(3-MTH) film changed from reddish brown to bluish green. Water droplets applied to this film were rapidly absorbed. (c) UV/vis measurements of the (reddish brown line) dedoped and (bluish green line) doped PEDOT-P(3-MTH) film.

shown in Figure 4c, the reversible wettability switching process could be repeated several times in this system.

In addition, the wetting behavior is dependent on the doping level of the PEDOT-P(3-MTH), which may be precisely controlled by adjusting the potential. A plot of WCA as a function of the potential from  $-0.2$  to  $+1.2$  V is shown in Figure 5a, which confirms the potential-dependent wettability switching of PEDOT-P(3-MTH). The WCA remained almost unchanged when the potential was increased from  $-0.2$  to  $+0.6$  V. During doping, PEDOT moieties in PEDOT-P(3-MTH) were oxidized, while P(3-MTH) moieties remained at a low

oxidation level (Figure 5b and Figure S4, Supporting Information). This behavior implies that the doping level of the PEDOT moieties does not significantly influence the WCA of the film. However, a rapid decrease in WCA from more than  $150^\circ$  to ca.  $0^\circ$  occurred when the applied potential was increased from  $+0.6$  to  $+1.0$  V. This decrease in WCA corresponds mainly to the oxidation of surface P(3-MTH) moieties in PEDOT-P(3-MTH). Therefore, the wettability of PEDOT-P(3-MTH) strongly depends on the doping level of the surface P(3-MTH) moieties. When the potential exceeded  $+1.0$  V, the superhydrophilic state of PEDOT-P(3-MTH) was

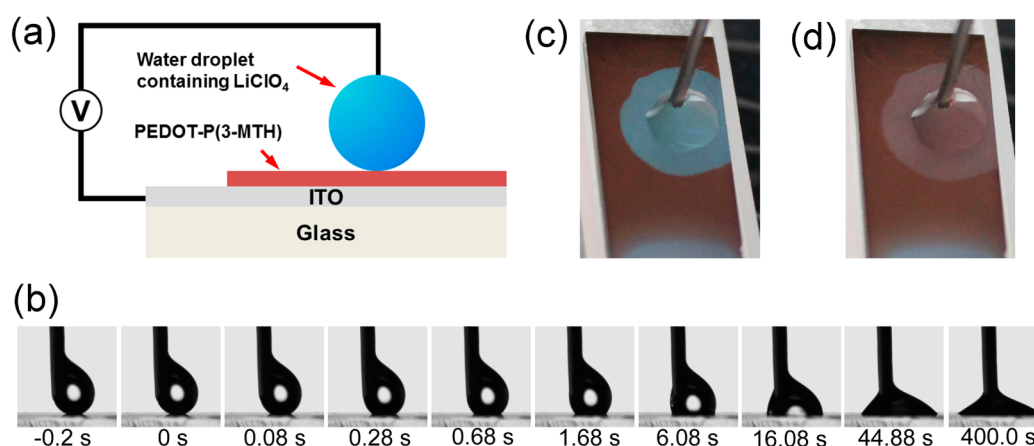


**Figure 8.** (a) Illustration of electro-wetting device. (b) The wettability change (in WCA) of the PEDOT–P(3-MTH) film with time prolonging when a potential of +1.5 V was applied between the water droplet (15  $\mu$ L) containing 0.2 M LiClO<sub>4</sub> and the film. (c) Formation of electro-wetting ring after applying the potential of +1.5 V for 400 s. (d) The color of the wetting ring changes from bluish green to reddish brown when the reverse potential of –1.5 V is applied for 10 s.

formed. When a gradually reducing potential from +1.2 to –0.2 V was applied to the doped PEDOT–P(3-MTH), a similar curve of WCA versus potential was produced. These observations further indicated that the water contact angle could be reversibly regulated by precisely controlling the applied potential.

**3.4. Effect of Electrolyte on Wettability Switching.** To investigate the effect of electrolyte on the wettability of the conductive film, we also doped and dedoped PEDOT–P(3-MTH) film in a 0.2 M TAHFP/ACN solution. It exhibits a similar electrochemical activity (Figure 6a). In this electrolyte solution system, the counterion PF<sub>6</sub><sup>–</sup> can be introduced into the polythiophene backbones under the doped potential of +1.6 V. Different with the dopant of LiClO<sub>4</sub>, the PEDOT–P(3-MTH) film processes a higher oxidation potential in this system than that in 0.2 M LiClO<sub>4</sub>/ACN solution. Furthermore, the film doped with TAHFP did not exhibit superhydrophilicity, but had a small WCA of about 15.5°. Upon the potential of –0.2 V in this electrolyte system, the film can recover its superhydrophobic surface with a WCA of about 155.5° (Figure 6b). Thus, the film in the TAHFP/ACN solution system only has a reversible wettability switching between superhydrophobicity and hydrophilicity. This may be due to a modest hydrophilicity of PF<sub>6</sub><sup>–</sup>.

**3.5. Photoelectric Properties and Wettability.** The wettability transition between superhydrophobicity and superhydrophilicity is accompanied by a change in the spectral properties of PEDOT–P(3-MTH), as manifested in electrochromism of the film (Figure 7). The dedoped PEDOT–P(3-MTH) film showed a reddish brown surface on which water droplets were nearly spherical in shape (Figure 7a). After doping, the film became bluish green, and water droplets applied to the surface could rapidly spread into the film (Figure 7b). The bluish green color of the doped film did not fade, even if it was immersed in water for 10 min (Figure S5, Supporting Information). The spectroelectrochemistry of PEDOT–P(3-MTH) (Figure 7c) was examined by using a UV/vis spectrophotometer coupled with an electrochemical analyzer. Upon dedoping at –0.2 V, the PEDOT–P(3-MTH) film showed a strong absorption maximum at 507 nm with a weak shoulder peak, which could be attributed to the  $\pi$ – $\pi^*$  transition absorption of the thiophene rings in the PEDOT and P(3-

MTH) moieties. As a result, the film has a reddish brown color.<sup>41</sup> Upon doping at +1.2 V, the PEDOT–P(3-MTH) film showed a red-shift in its absorption because of the absorption of charge carrier bands,<sup>41</sup> giving rise to a bluish green color. Therefore, the PEDOT–P(3-MTH) film exhibited an electro-responsive, switchable wettability surface, the wettability state of which could be easily judged by its color.

**3.6. Electro-Wetting Device.** On the basis of the electro-wetting properties of the PEDOT–P(3-MTH) film, we designed a simple in situ electro-wetting device to explore the application of such a conductive polymer film (Figure 8a).<sup>44,45</sup> At the beginning, a water droplet (15  $\mu$ L) containing 0.2 M LiClO<sub>4</sub> on the film in the electro-wetting device exhibits a high contact angle greater than 150° (Figure 8b, first image). When we applied the potential of +1.5 V between the water droplet and the superhydrophobic film, the wettability of the film underneath the water continuously transformed from superhydrophobicity to hydrophobicity, with time prolonging (Figure 8b). If we ignore the effect of the electrolyte on WCA, we believe the water droplet on this film to be in Cassie's superhydrophobic state, because there was only little liquid–solid contact area due to the presence of an air cushion.<sup>31,32,38</sup> When a potential of +1.5 V was applied, migration of the charge carrier (including an electron moving out and ClO<sub>4</sub><sup>–</sup> moving in) on the liquid–solid contact location occurred, accompanying an electrochemical (doped) process. The change in the chemical component on the liquid–solid contact location leads to the wettability change. The water droplet permeated the porous film under potential (Figure 8b and Movie S2, Supporting Information). After we applied potential for 400 s, the water droplet on the film had a small contact angle less than 35° (Figure 8b, last image). Figure 8c shows a large wetting ring after the voltage was applied for 400 s. In the wetting ring, the film experienced complete wetting. If we applied a reverse potential of –1.5 V for 10 s, the color of the wetting ring changed from bluish green to reddish brown (Figure 8d). However, its wettability state was not recovered in the acceptable range of time.

## 4. CONCLUSION

An electro-responsive porous structured polythiophene film showing reversible switching of wettability between super-

hydrophobicity and superhydrophilicity has been successfully prepared. The highly porous polythiophene film, composed of a layer of P(3-MTH) applied to underlying PEDOT, was synthesized on an ITO substrate by a two-step electro-deposition method. The wettability switching of this film between superhydrophobicity and superhydrophilicity could be realized by electrochemical doping and dedoping. The superhydrophobicity with WCA > 150° in the dedoped state and superhydrophilicity with WCA ≈ 0° in the doped state of the polythiophene film could be repeatedly attained by alternately applying potentials of -0.2 and +1.2 V, respectively. Notably, the wettability state could also be judged by the color of the film. A simple device was designed for exhibition of its electro-wetting property. This large-area smart surface with rapid wettability switching may potentially be applied in academic and industrial contexts.

## ■ ASSOCIATED CONTENT

### ■ Supporting Information

Successive CV curves of the electrodeposition of P(3-MTH), PEDOT, and PEDOT-P(3-MTH) films; wettability change of P(3-MTH) on ITO glass; photograph of the doped film immersed in water; and movies of the moving water droplet and electro-wetting test. This material is available free of charge via the Internet at <http://pubs.acs.org>.

## ■ AUTHOR INFORMATION

### Corresponding Author

\*E-mail: [qhlu@sjtu.edu.cn](mailto:qhlu@sjtu.edu.cn).

### Notes

The authors declare no competing financial interest.

## ■ ACKNOWLEDGMENTS

The authors are grateful for financial support from the National Science Foundation of China (21374060 and 51173103), 973 Projects (2012CB933803 and 2014CB643605), and the National Science Fund for Distinguished Young Scholars (50925310).

## ■ REFERENCES

- (1) Liu, K. S.; Jiang, L. Bio-Inspired Self-Cleaning Surfaces. *Annu. Rev. Mater. Res.* **2012**, *42*, 231–263.
- (2) Yohe, S. T.; Colson, Y. L.; Grinstaff, M. W. Superhydrophobic Materials for Tunable Drug Release: Using Displacement of Air to Control Delivery Rates. *J. Am. Chem. Soc.* **2012**, *134*, 2016–2019.
- (3) Zhou, H.; Wang, H. X.; Niu, H. T.; Gestos, A.; Wang, X. G.; Lin, T. Fluoroalkylsilane-Modified Silicone Rubber/Nanoparticle Composite: A Super-Durable, Robust Superhydrophobic Fabric Coating. *Adv. Mater.* **2012**, *24*, 2409–2412.
- (4) Liu, M. J.; Zheng, Y. m.; Zhai, J.; Jiang, L. Bioinspired Super-Antiwetting Interfaces with Special Liquid–Solid Adhesion. *Acc. Chem. Res.* **2010**, *43*, 368–377.
- (5) Deng, X.; Mammen, L.; Butt, H. J.; Vollmer, D. Candle Soot as a Template for a Transparent Robust Superamphiphobic Coating. *Science* **2012**, *335*, 67–70.
- (6) Barthlott, W.; Neinhuis, C. Purity of the Sacred Lotus, or Escape from Contamination in Biological Surfaces. *Planta* **1997**, *202*, 1–8.
- (7) Wu, Z. P.; Xu, Q. F.; Wang, J. N.; Ma, J. Preparation of Large-Area Double-Walled Carbon Nanotube Macro-Films with Self-Cleaning Properties. *J. Mater. Sci. Technol.* **2010**, *26*, 20–26.
- (8) Lai, Y. K.; Tang, Y. X.; Gong, J. J.; Gong, D. G.; Chi, L. F.; Lin, C. J.; Chen, Z. Transparent Superhydrophobic/Superhydrophilic TiO<sub>2</sub>-Based Coatings for Self-Cleaning and Anti-Fogging. *J. Mater. Chem.* **2012**, *22*, 7420–7426.
- (9) Yao, L.; He, J. H. Broadband Antireflective Superhydrophilic Thin Films with Outstanding Mechanical Stability on Glass Substrates. *Chin. J. Chem.* **2014**, *32*, 507–512.
- (10) Tian, D. L.; Zhai, J.; Song, Y. L.; Jiang, L. Photoelectric Cooperative Induced Wetting on Aligned-Nanopore Arrays for Liquid Reprography. *Adv. Funct. Mater.* **2011**, *21*, 4519–4526.
- (11) Mertaniemi, H.; Jokinen, V.; Sainiemi, L.; Franssila, S.; Marmur, A.; Ikkala, O.; Ras, R. H. A. Superhydrophobic Tracks for Low-Friction, Guided Transport of Water Droplets. *Adv. Mater.* **2011**, *23*, 2911–2914.
- (12) Ueda, E.; Levkin, P. A. Emerging Applications of Superhydrophilic–Superhydrophobic Micropatterns. *Adv. Mater.* **2013**, *25*, 1234–1247.
- (13) Liu, Q. Y.; Gao, L.; Jiang, L. Biomimetic Preparation and Multi-Scale Microstructures of Nano-Silica/Polyurethane Elastomeric Fibers. *Prog. Nat. Sci.: Mater. Int.* **2013**, *23*, 532–542.
- (14) Feng, X. J.; Feng, L.; Jin, M. H.; Zhai, J.; Jiang, L.; Zhu, D. B. Reversible Super-Hydrophobicity to Super-Hydrophilicity Transition of Aligned ZnO Nanorod Films. *J. Am. Chem. Soc.* **2004**, *126*, 62–63.
- (15) Lim, H. S.; Han, J. T.; Kwak, D.; Jin, M. H.; Cho, K. Photoreversibly Switchable Superhydrophobic Surface with Erasable and Rewritable Pattern. *J. Am. Chem. Soc.* **2006**, *128*, 14458–14459.
- (16) Lim, H. S.; Kwak, D.; Lee, D. Y.; Lee, S. G.; Cho, K. UV-Driven Reversible Switching of a Roselike Vanadium Oxide Film between Superhydrophobicity and Superhydrophilicity. *J. Am. Chem. Soc.* **2007**, *129*, 4128–4129.
- (17) Xu, L. B.; Chen, W.; Mulchandani, A.; Yan, Y. S. Reversible Conversion of Conducting Polymer Films from Superhydrophobic to Superhydrophilic. *Angew. Chem., Int. Ed.* **2005**, *44*, 6009–6012.
- (18) Xia, F.; Feng, L.; Wang, S. T.; Sun, T. L.; Song, W. L.; Jiang, W. H.; Jiang, L. Dual-Responsive Surfaces that Switch between Superhydrophilicity and Superhydrophobicity. *Adv. Mater.* **2006**, *18*, 432–436.
- (19) Lim, H. S.; Lee, S. G.; Lee, D. H.; Lee, D. Y.; Lee, S.; Cho, K. Superhydrophobic to Superhydrophilic Wetting Transition with Programmable Ion-Pairing Interaction. *Adv. Mater.* **2008**, *20*, 4438–4441.
- (20) Hou, W. X.; Wang, Q. H. UV-Driven Reversible Switching of a Polystyrene/Titania Nanocomposite Coating between Superhydrophobicity and Superhydrophilicity. *Langmuir* **2009**, *25*, 6875–6879.
- (21) Yang, J.; Zhang, Z. Z.; Men, X. H.; Xu, X. H.; Zhu, X. T. Reversible Superhydrophobicity to Superhydrophilicity Switching of a Carbon Nanotube Film via Alternation of UV Irradiation and Dark Storage. *Langmuir* **2010**, *26*, 10198–10202.
- (22) Xia, F.; Zhai, J.; Jiang, L. The Fabrication and Switchable Superhydrophobicity of TiO<sub>2</sub> Nanorod Films. *Angew. Chem., Int. Ed.* **2005**, *44*, 5115–5118.
- (23) Yu, X.; Wang, Z. Q.; Jiang, Y. G.; Shi, F.; Zhang, X. Reversible pH-Responsive Surface: From Superhydrophobicity to Superhydrophilicity. *Adv. Mater.* **2005**, *17*, 1289–1293.
- (24) Zhu, Y.; Feng, L.; Xia, F.; Zhai, J.; Wan, M. X.; Jiang, L. Chemical Dual-Responsive Wettability of Superhydrophobic PANI-PAN Coaxial Nanofibers. *Macromol. Rapid Commun.* **2007**, *28*, 1135–1141.
- (25) Lahann, J.; Mitragotri, S.; Tran, T. N.; Kaido, H.; Sundaram, J.; Choi, I. S.; Hoffer, S.; Somorjai, G. A.; Langer, R. A Reversibly Switching Surface. *Science* **2003**, *299*, 371–374.
- (26) Xia, F.; Jiang, L. Bio-Inspired, Smart, Multiscale Interfacial Materials. *Adv. Mater.* **2008**, *20*, 2842–2858.
- (27) Pernites, R. B.; Ponnappati, R. R.; Advincula, R. C. Superhydrophobic–Superoleophilic Polythiophene Films with Tunable Wetting and Electrochromism. *Adv. Mater.* **2011**, *23*, 3207–3213.
- (28) Manukyan, G.; Oh, J. M.; van den Ende, D.; Lammertink, R. G. H.; Mugele, F. Electrical Switching of Wetting States on Superhydrophobic Surfaces: A Route towards Reversible Cassie-to-Wenzel Transitions. *Phys. Rev. Lett.* **2011**, *106*, 014501.
- (29) Darmanin, T.; de Givenchy, E. T.; Amigoni, S.; Guittard, F. Superhydrophobic Surfaces by Electrochemical Processes. *Adv. Mater.* **2013**, *25*, 1378–1394.

- (30) Xu, L. B.; Chen, Z. W.; Chen, W.; Mulchandani, A.; Yan, Y. S. Electrochemical Synthesis of Perfluorinated Ion Doped Conducting Polyaniline Films Consisting of Helical Fibers and Their Reversible Switching between Superhydrophobicity and Superhydrophilicity. *Macromol. Rapid Commun.* **2008**, *29*, 832–838.
- (31) Cassie, A. B. D.; Baxter, S. Wettability of Porous Surfaces. *Trans. Faraday Soc.* **1944**, *40*, 546–551.
- (32) Lafuma, A.; Quéré, D. Superhydrophobic States. *Nat. Mater.* **2003**, *2*, 457–460.
- (33) Li, C.; Guo, R. W.; Jiang, X.; Hu, S. X.; Li, L.; Cao, X. Y.; Yang, H.; Song, Y. L.; Ma, Y. M.; Jiang, L. Reversible Switching of Water-Droplet Mobility on a Superhydrophobic Surface based on a Phase Transition of a Side-Chain Liquid-Crystal Polymer. *Adv. Mater.* **2009**, *21*, 4254–4258.
- (34) Leon, A. C. C.; Pernites, R. B.; Advincula, R. C. Superhydrophobic Colloidally Textured Polythiophene Film as Superior Anticorrosion Coating. *ACS Appl. Mater. Interfaces* **2012**, *4*, 3169–3176.
- (35) Zhang, Z. P.; Qu, L. T.; Shi, G. Q. Fabrication of Highly Hydrophobic Surfaces of Conductive Polythiophene. *J. Mater. Chem.* **2003**, *13*, 2858–2860.
- (36) Lin, P.; Yan, F.; Chan, H. L. W. Improvement of the Tunable Wettability Property of Poly(3-alkylthiophene) Films. *Langmuir* **2009**, *25*, 7465–7470.
- (37) Xu, L. Y.; Lu, X. M.; Li, M.; Lu, Q. H. Reversible Switching of Water-Droplet Adhesion on a Superhydrophobic Polythiophene Surface. *Adv. Mater. Interfaces* **2014**, 10.1002/admi.201400011.
- (38) Tuteja, A.; Choi, W.; Ma, M.; Mabry, J. M.; Mazzella, S. A.; Rutledge, G. C.; McKinley, G. H.; Cohen, R. E. Designing Superoleophobic Surfaces. *Science* **2007**, *318*, 1618–1622.
- (39) Darmanin, T.; de Givenchy, E. T.; Amigoni, S.; Guittard, F. Hydrocarbon versus Fluorocarbon in the Electrodeposition of Superhydrophobic Polymer Films. *Langmuir* **2010**, *26*, 17596–17602.
- (40) Dang, M. T.; Hirsch, L.; Wantz, G.; Wuest, J. D. Controlling the Morphology and Performance of Bulk Heterojunctions in Solar Cells. Lessons Learned from the Benchmark Poly(3-hexylthiophene):[6,6]-Phenyl-C<sub>61</sub>-Butyric Acid Methyl Ester System. *Chem. Rev.* **2013**, *113*, 3734–3765.
- (41) Xu, L. Y.; Zhao, J. S.; Cui, C. S.; Liu, R. M.; Liu, J. F.; Wang, H. S. Electrosynthesis and Characterization of an Electrochromic Material from Poly(1,4-bis(2-thienyl)benzene) and its Application in Electrochromic Devices. *Electrochim. Acta* **2011**, *56*, 2815–2822.
- (42) Bico, J.; Thiele, U.; Quéré, D. Wetting of Textured Surfaces. *Colloids Surf., A* **2002**, *206*, 41–46.
- (43) Rafiee, J.; Rafiee, M. A.; Yu, Z. Z.; Koratkar, N. Superhydrophobic to Superhydrophilic Wetting Control in Graphene Films. *Adv. Mater.* **2010**, *22*, 2151–2154.
- (44) Dhindsa, M. S.; Smith, N. R.; Heikenfeld, J. Reversible Electrowetting of Vertically Aligned Superhydrophobic Carbon Nanofibers. *Langmuir* **2006**, *22*, 9030–9034.
- (45) Krupenkin, T. N.; Taylor, J. A.; Schneider, T. M.; Yang, S. From Rolling Ball to Complete Wetting: The Dynamic Tuning of Liquids on Nanostructured Surfaces. *Langmuir* **2004**, *20*, 3824–3827.